



# Cavitating Langmuir Turbulence in the Terrestrial Aurora

B. Isham, M. T. Rietveld, P. Guio, F. R. E. Forme, T. Grydeland, E. Mjølhus

## ► To cite this version:

B. Isham, M. T. Rietveld, P. Guio, F. R. E. Forme, T. Grydeland, et al.. Cavitating Langmuir Turbulence in the Terrestrial Aurora. *Physical Review Letters*, 2012, 108, pp.105003. <10.1103/PhysRevLett.108.105003>. <hal-00557486>

**HAL Id: hal-00557486**

**<https://hal.science/hal-00557486v1>**

Submitted on 11 May 2023

**HAL** is a multi-disciplinary open access archive for the deposit and dissemination of scientific research documents, whether they are published or not. The documents may come from teaching and research institutions in France or abroad, or from public or private research centers.

L'archive ouverte pluridisciplinaire **HAL**, est destinée au dépôt et à la diffusion de documents scientifiques de niveau recherche, publiés ou non, émanant des établissements d'enseignement et de recherche français ou étrangers, des laboratoires publics ou privés.



HAL Authorization

## Cavitating Langmuir Turbulence in the Terrestrial Aurora

B. Isham,<sup>1,\*</sup> M. T. Rietveld,<sup>2</sup> P. Guio,<sup>3</sup> F. R. E. Forme,<sup>4</sup> T. Grydeland,<sup>5</sup> and E. Mjølhus<sup>6</sup>

<sup>1</sup>*Department of Electrical and Computer Engineering, Interamerican University of Puerto Rico, Bayamón, Puerto Rico 00957, USA*

<sup>2</sup>*European Incoherent Scatter Scientific Association, 9027 Ramfjordbotn, Norway*

<sup>3</sup>*Department of Physics and Astronomy, University College London, London, WC1E 6BT, United Kingdom*

<sup>4</sup>*Centre d'Étude Spatiale des Rayonnements, 31028 Toulouse, France*

<sup>5</sup>*Northern Research Institute Tromsø, Postboks 6434 Forskningsparken, 9294 Tromsø, Norway*

<sup>6</sup>*Department of Mathematics and Statistics, University of Tromsø, 9037 Tromsø, Norway*

(Received 2 November 2010; published 8 March 2012)

Langmuir cavitons have been artificially produced in Earth's ionosphere, but evidence of naturally occurring cavitation has been elusive. By measuring and modeling the spectra of electrostatic plasma modes, we show that natural cavitating, or strong, Langmuir turbulence does occur in the ionosphere, via a process in which a beam of auroral electrons drives Langmuir waves, which in turn produce cascading Langmuir and ion-acoustic excitations and cavitating Langmuir turbulence. The data presented here are the first direct evidence of cavitating Langmuir turbulence occurring naturally in any space or astrophysical plasma.

DOI: 10.1103/PhysRevLett.108.105003

PACS numbers: 94.05.Lk, 94.05.Fg, 94.05.Pt, 94.20.wj

Langmuir turbulence is known to occur in controlled laboratory [1,2] and space plasma experiments [3–5] and is thought to occur naturally in a variety of space and astrophysical plasmas, including pulsar magnetospheres [6], the solar corona [7], the interplanetary medium [8], planetary foreshocks [9], the terrestrial magnetosphere [10], and the ionosphere [11–13]. In its most developed form, this turbulence contains electron Langmuir modes trapped in dynamic density depressions known as cavitons [14–16]. Cavitons have been shown to be artificially produced in Earth's ionosphere during high-power radio-wave pumping experiments as deduced from radar spectra containing simultaneously excited up- and downshifted Langmuir and ion-acoustic lines plus a central peak due to cavitation [3–5], but evidence of naturally occurring cavitation has until now been elusive.

Between 18:00 and 21:00 UT on 11 and 12 November 1999, a measurement program designed to detect both ion-acoustic and Langmuir modes was run on the European Incoherent Scatter Scientific Association (EISCAT) 224-MHz radar located near Tromsø in northern Norway (local standard time in Norway is UT plus 1 h). The principal objectives were to observe enhanced waves stimulated by high-power radio-wave pumping and, in the event of auroral activity, to gather data on natural energetic waves [17]. On both nights, conditions were disturbed, and enhanced echoes were detected, the strongest being on 11 November between 18:18:30 and 18:21:30 UT, during the passage of an aurora through the vertically directed radar beam. Figure 1 presents parameters derived from the ion-acoustic backscatter between 18:15 and 18:28 UT, during the most intense auroral event. Figure 2 shows the intensities of Langmuir and ion-acoustic backscatter as a function of height and time. The prominent features occurring between 18:18:30 and 18:20:30 UT and at 18:23:30 UT near 300

and 250 km altitude, respectively, are backscatter associated with the aurora and are the most energetic natural events observed on either night. Two other events occurred later that evening and two more on the following evening. Weak ion-acoustic enhancements occurred during each event; the Langmuir enhancements, however, are always stronger. Figure 3 shows up- and downshifted spectral lines, or “shoulders,” which are produced by Doppler-shifted backscatter from the down- and up-going ion-acoustic waves, respectively. The shoulders are strongly enhanced, indicating that the waves are nonlinearly amplified. In addition, there is a strong central peak, a feature not present in thermal-level spectra.

The results of a computation made for plasma parameters matching those which occurred during this observation are shown in Fig. 4. A numerical code incorporating a one-dimensional periodic version of the Zakharov equations was used [13,18], capable of producing the full range of cascading (sometimes called weak), coexistence (transitional), and cavitating (strong) Langmuir turbulence. Energy was supplied by a downward-going flux, or beam, of electrons [19], which excites a Langmuir “pump” wave via the bump-on-tail instability. In the cascading turbulence scenario [20], the Langmuir wave then undergoes parametric decay into daughter Langmuir and ion-acoustic waves. These waves, however, exist only within two relatively narrow bands of wave numbers: the Langmuir band defined by the driving beam (see the caption to Fig. 4) and the ion-acoustic band at about twice that value. Furthermore, a radar sees only the wave number that matches the Bragg scattering condition for the radar wavelength. This means that, for beam-driven cascading turbulence, a radar will see either enhanced Langmuir waves or enhanced ion-acoustic waves, but both may be seen simultaneously only when the velocity spread of the beam is

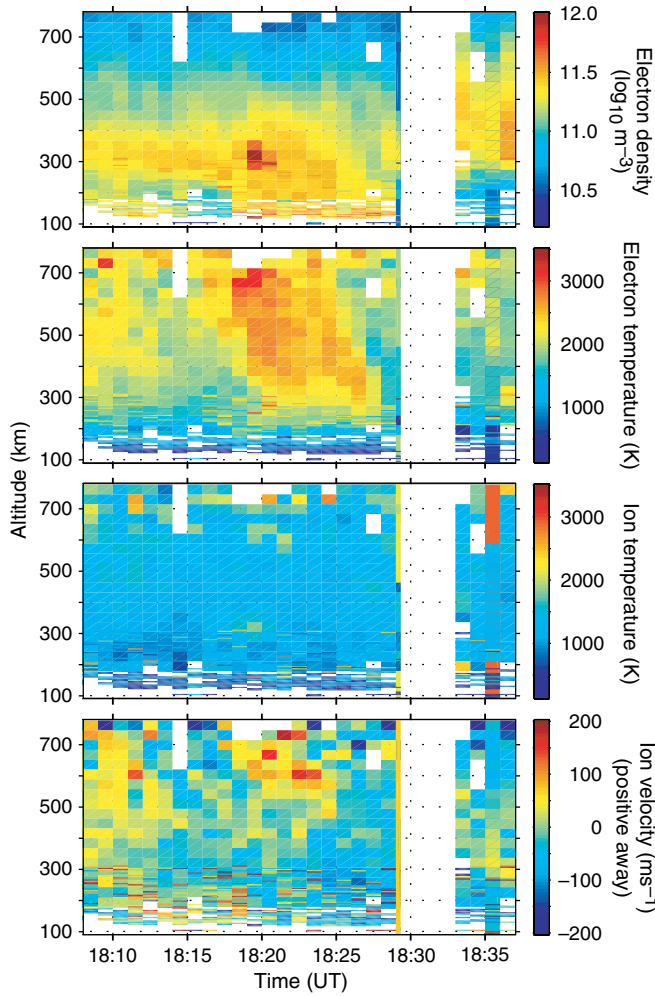


FIG. 1 (color online). Background ionospheric parameters measured during the most prominent auroral event. The panels show, from top to bottom, electron density, electron temperature, ion temperature, and vertical ion velocity (positive indicates motion away from the observer) at 1-min time resolution. Typical auroral plasma signatures can be seen, namely, a sharp increase in electron density localized in time and space, a corresponding increase in electron temperature, localized small increases in ion temperature, and, in the velocity plot, high-altitude ion outflow to space [28,29].

sufficiently broad, approaching the absolute velocity of the beam itself. Cavitating turbulence is different in that enhanced wave modes cover a range of  $k$  space which extends broadly on both sides of the wave number of the pump wave irrespective of the beam velocity breadth. In the coexistence or transitional case, the wave number spectrum extends below the pump wave number to zero, but dies out rapidly for Langmuir wave numbers greater than the Langmuir pump and for ion-acoustic wave numbers greater than twice the Langmuir pump.

In the simulations presented in Fig. 4, several different beam energies are modeled, each capable of producing cavitating turbulence, and the spectra are those which

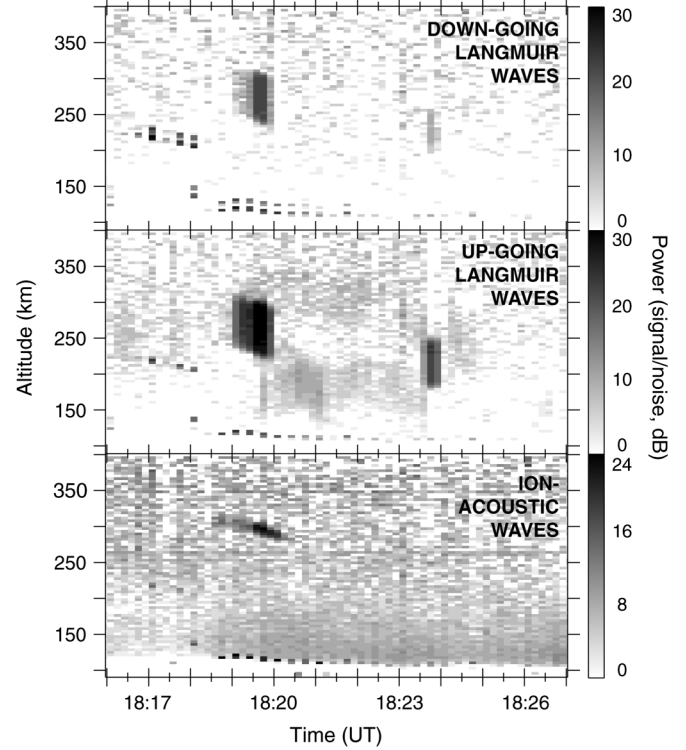


FIG. 2. Incoherent scatter intensity profiles from up- and down-going Langmuir and ion-acoustic waves recorded during the auroral event discussed in Fig. 1. Four distinct sources of scattering can be identified. (i) The dark background in the ion-acoustic channel is backscatter from thermal-level waves. (ii) The relatively faint bands in the down-going and, more prominently, up-going Langmuir channels correspond to 3 and 5 MHz Langmuir waves weakly enhanced by low energy, direct and backscattered diffuse electron precipitation associated with the aurora. (iii) The repeated 10-s-long enhancements seen in all three channels at about 225 and 125 km before and after 18:18:30, respectively, are backscatter from waves enhanced by experimental 4.04-MHz high-power radio-wave transmissions [17]. (iv) The intense features occurring between 18:18:30 and 18:20:30 UT near 300 km and at 18:23:30 UT near 250 km are backscatter associated with the aurora. The top edges of the Langmuir enhancements give the approximate altitudes of the enhanced backscatter. Uncoded 420- and 25- $\mu$ s pulses were used to measure the Langmuir and ion-acoustic backscatter, respectively.

would be seen by a radar of the same wavelength as was used for the observations; however, the beam parameters were chosen so that the Langmuir and ion-acoustic wave numbers for cascading turbulence would not match that of the radar. The coincident enhancement in space and time of both ion-acoustic and Langmuir backscatter at a single radar wave number is a prediction characteristic of cavitating Langmuir turbulence and constitutes critical evidence for its occurrence [13,14].

A second key feature of this observation lies in the shape of the ion-acoustic spectra, which consists of enhanced up- and downshifted shoulders and an enhanced central peak,

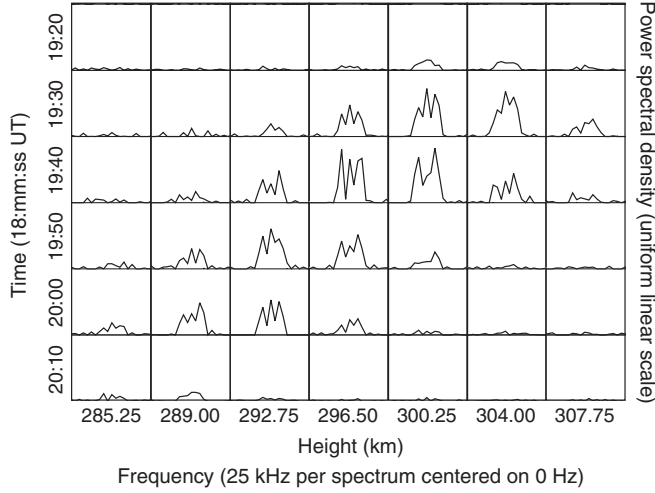


FIG. 3. Power spectral densities of the naturally enhanced ion-acoustic backscatter showing enhanced shoulders and enhanced central peaks at 2-kHz frequency and 3.75-km range resolution. A 475- $\mu$ s phase-coded pulse with a 25- $\mu$ s baud was used. The change in enhancement height with time is a result of the vertical pointing of the radar, while the auroral structure is oriented along the geomagnetic field, tilted 13° south of vertical, and drifting south; this effect can also be seen in Fig. 2. The progression from higher to lower heights with time corresponds to a drift velocity of about 80 m/s.

shown in Fig. 3. The observed spectra match the computed spectra in Fig. 4 very well. Enhanced shoulders are a standard feature of all past observations of naturally enhanced ion-acoustic backscatter [21], but only one past result shows an enhanced ion-acoustic spectrum with a central peak [22]. The appearance of the non-Doppler-shifted central peak indicates the presence of meter-scale, nonpropagating density wells known as cavitons. A central peak is not a necessary feature of cavitating turbulence but will occur when the spacing between the cavitons matches the Bragg condition of the radar. The spacing, in turn, is roughly proportional to the inverse square root of the energy density of the primary Langmuir waves or, in turn, of the pump beam [13,23]. This is not likely to be seen in all observations, both because of the matching requirement and because a relatively high beam energy density is required, which is most likely to be observable by using long wavelengths such as in the observations reported here and previously [22].

Many other features of the observations may also be explained by the cavitating turbulence model. (i) Six events were observed, four on the 11th and two on the 12th, and both Langmuir and ion-acoustic enhancements exist in all cases, but in all events the ion-acoustic enhancement is weaker. This agrees with the computed examples. (ii) The measured backscatter intensity in the down-going Langmuir channels is weaker than the up-going. Similar differences can be seen in the computed spectra. For the case of 18 eV, the radar sees down-going Langmuir modes

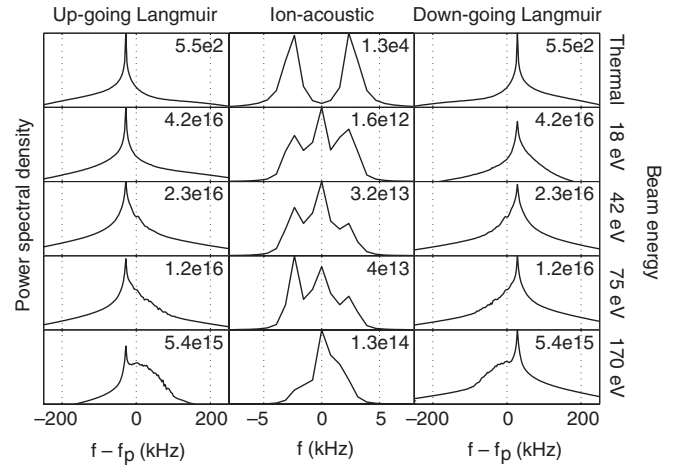


FIG. 4. Results from a 1D simulation made for plasma parameters matching those during this observation and with a downward-going beam of electrons at beam energies of 18, 42, 75, and 170 eV. The beam creates a bump-on-tail distribution which excites Langmuir waves according to the resonance condition  $v_b \approx \lambda_L f_L$ , where  $v_b$  is the beam velocity and  $\lambda_L$  and  $f_L$  are the Langmuir wavelength and frequency, respectively. The spectra of up- and down-going Langmuir and ion-acoustic waves were calculated for a wavelength of 0.67 m, matching the Bragg backscatter condition of the radar. Both the precipitating electron beam and the thermal background were included in the driving terms. The beam velocity spread ratio  $\Delta v_b/v_b$  is 0.3 in all cases, where  $\Delta v_b$  is the velocity spread. The beam density ratio  $n_b/n_p$  is  $2 \times 10^{-5}$ , where  $n_b$  is the beam density and  $n_p$  is the density of the surrounding plasma,  $3 \times 10^{11} \text{ m}^{-3}$ , as determined from the 5-MHz frequency of the enhanced Langmuir modes. The electron collision frequency is  $200 \text{ s}^{-1}$ . These parameters are well within the ranges known to occur in the auroral ionosphere [19]. The peak value of each spectrum is given at the top right of each panel. The Langmuir spectra are shown on identical log scales with arbitrary but equal reference levels and with a minimum value  $10^{-6}$  that of the maximum; the ion-acoustic spectra are shown on a linear scale in arbitrary units with a minimum value of zero.

at a wave number corresponding to the negative, or damping, slope of the velocity distribution function of the down-going beam, and heavy damping is seen. For wave numbers on the positive slope of the beam, the opposite will occur. (iii) In five of our cases, the ion-acoustic enhancement disappears before, or at the same time as, the Langmuir enhancements (within the 10-s time resolution of the observations). However, in our strongest event, at 18:18:30 on the 11th, enhanced ion-acoustic backscatter is seen before and after the enhanced Langmuir backscatter. In this case, it is possible that the turbulence develops from coexistence to cavitating and back again as the driving beam grows and then decays. In the coexistence regime, Langmuir mode wave numbers are cut off at a value roughly half that of the ion-acoustic mode, so the radar may see only the ion-acoustic enhancement until the cavitating turbulence is fully developed. A strong event would also cause greater



electron heating, reducing damping of ion-acoustic modes and contributing to a longer ion-acoustic enhancement. (iv) The relationship between beam energy and ion-acoustic damping can also account for the relatively strong ion-acoustic enhancement after 18:20:00 UT: The electrons had been heated during the event and the ion-acoustic damping rate reduced, allowing the ion-acoustic backscatter to remain strong even as the drive began to weaken.

A significant feature in the computed Langmuir spectrum at 170 eV, and very weakly at 42 and 75 eV, is the appearance of a broad spectrum at and near the cold plasma frequency. This feature, which is not resolvable in the radar measurements presented here, is due to Langmuir waves trapped in cavitons. It appears after a sufficient period of pumping at a sufficiently high level. The central peak and the broad spectrum, both due to cavitation, may be seen under somewhat different circumstances: The central peak requires a beam energy density that allows the caviton spacing to match the radar Bragg condition, while the broad spectrum requires a fixed electron density with a beam velocity high enough and beam duration long enough to allow formation of trapped Langmuir waves matching the radar Bragg condition. Both are seen in high-power radio-wave experiments [5], in which a fixed pump frequency substitutes for a fixed electron density.

The data presented here provide the first direct evidence of naturally occurring cavitating Langmuir turbulence, thought to be important in space and astrophysical plasmas as varied as pulsar magnetospheres and Earth's ionosphere [6–14]. Further observations of Langmuir turbulence in the ionosphere may yield advances in our understanding of suprathermal electron distributions [24], naturally enhanced ion-acoustic waves [13,20], natural ionospheric radio emissions [25], anomalous resistivity [26,27], and auroral currents and dark aurora [28].

EISCAT is supported by research organizations in China, Finland, France, Germany, Japan, Norway, Russia, Sweden, Ukraine, and the United Kingdom. Support for B.I. and M.T.R. was provided in part, respectively, by U.S. Army Research Office Contract No. W911NF-07-1-0016 and by the Max-Planck-Institute for Aeronomy. Some of the calculations were performed on facilities provided by the Miracle Consortium, part of the DiRAC project funded by the United Kingdom Science and Technology Facilities Council. We thank César La Hoz for helping to arrange observation time on the EISCAT radar system, and we thank César La Hoz, Jim LaBelle, Kristina Lynch, Iver Cairns, Gerhard Haerendal, and two anonymous referees for constructive and helpful comments.

---

\*bisham@email.bc.inter.edu

[1] A. Y. Wong and P. Y. Cheung, *Phys. Rev. Lett.* **52**, 1222 (1984).

- [2] L. N. Vyacheslavov, V. S. Burmasov, I. V. Kandaurov, E. P. Kruglyakov, O. I. Meshkov, S. S. Popov, and A. L. Sanin, *Plasma Phys. Controlled Fusion* **44**, B279 (2002).
- [3] M. P. Sulzer and J. A. Fejer, *J. Geophys. Res.* **99**, 15 035 (1994).
- [4] B. Isham, C. La Hoz, M. T. Rietveld, T. Hagfors, and T. B. Leyser, *Phys. Rev. Lett.* **83**, 2576 (1999).
- [5] M. T. Rietveld, B. Isham, H. Kohl, C. La Hoz, and T. Hagfors, *J. Geophys. Res.* **105**, 7429 (2000).
- [6] E. Asseo and A. Porzio, *Mon. Not. R. Astron. Soc.* **369**, 1469 (2006).
- [7] A. L. Nulsen, I. H. Cairns, and P. A. Robinson, *J. Geophys. Res.* **112**, 5107 (2007).
- [8] P. J. Kellogg, K. Goetz, R. L. Howard, and S. J. Monson, *Geophys. Res. Lett.* **19**, 1303 (1992).
- [9] P. A. Robinson and I. H. Cairns, *Geophys. Res. Lett.* **22**, 2657 (1995).
- [10] K. Stasiewicz, B. Holback, V. Krasnoselskikh, M. Boehm, R. Boström, and P. M. Kintner, *J. Geophys. Res.* **101**, 21 515 (1996).
- [11] K. Papadopoulos and T. Coey, *J. Geophys. Res.* **79**, 674 (1974).
- [12] H. L. Rowland, J. G. Lyon, and K. Papadopoulos, *Phys. Rev. Lett.* **46**, 346 (1981).
- [13] P. Guio and F. Forme, *Phys. Plasmas* **13**, 122902 (2006).
- [14] P. A. Robinson, *Rev. Mod. Phys.* **69**, 507 (1997).
- [15] D. F. DuBois, H. A. Rose, and D. Russell, *Phys. Rev. Lett.* **66**, 1970 (1991).
- [16] D. F. DuBois, A. Hanssen, H. A. Rose, and D. Russell, *Phys. Fluids B* **5**, 2616 (1993).
- [17] M. T. Rietveld, B. Isham, T. Grydeland, C. La Hoz, T. B. Leyser, F. Honary, H. Ueda, M. Kosch, and T. Hagfors, *Adv. Space Res.* **29**, 1363 (2002).
- [18] V. E. Zakharov, *Sov. Phys. JETP* **35**, 908 (1972).
- [19] J. D. Williams, E. MacDonald, M. McCarthy, L. Peticolas, and G. K. Parks, *Ann. Geophys.* **24**, 1829 (2006).
- [20] F. R. E. Forme, *Ann. Geophys.* **17**, 1172 (1999).
- [21] F. Sedgemore-Schulthess and J.-P. St.-Maurice, *Surv. Geophys.* **22**, 55 (2001).
- [22] F. R. E. Forme, D. Fontaine, and J. E. Wahlund, *J. Geophys. Res.* **100**, 14 625 (1995).
- [23] M. Shen and D. R. Nicholson, *Phys. Fluids* **30**, 1096 (1987).
- [24] D. L. Matthews, M. Pongratz, and K. Papadopoulos, *J. Geophys. Res.* **81**, 123 (1976).
- [25] J. M. Hughes and J. LaBelle, *J. Geophys. Res.* **106**, 21 157 (2001).
- [26] K. Papadopoulos and T. Coey, *J. Geophys. Res.* **79**, 1558 (1974).
- [27] H. L. Rowland, K. Papadopoulos, and P. J. Palmadesso, *Geophys. Res. Lett.* **8**, 1257 (1981).
- [28] T. Grydeland, E. M. Blixt, U. P. Løvhaug, T. Hagfors, C. L. Hoz, and T. S. Trondsen, *Ann. Geophys.* **22**, 1115 (2004).
- [29] E. M. Blixt, T. Grydeland, N. Ivchenko, T. Hagfors, C. L. Hoz, B. S. Lanchester, U. P. Løvhaug, and T. S. Trondsen, *Ann. Geophys.* **23**, 3 (2005).